Current Problems in Cancer 47 (2023) 101007

Contents lists available at ScienceDirect

Current Problems in Cancer

journal homepage: www.elsevier.com/locate/cpcancer

The prognostic value of FIGO staging defined by combining MRI and [^{18}F]FDG PET/CT in patients with locally advanced cervical cancer

Stefano Raffa[a,*], Francesco Lanfranchi[b,*], Camilla Satragno[c], Flavio Giannelli[d], Michela Marcenaro[d], Angela Coco[b], Sofia Elizabeth Cena[b], Luca Sofia[b], Cecilia Marini[a,e], Serafina Mammoliti[f], Alessia Levaggi[g], Alberto Stefano Tagliafico[b,h], Gianmario Sambuceti[a,b], Salvina Barra[d], Silvia Morbelli[a,b], Liliana Belgioia[b,d,**], Matteo Bauckneht[a,b,**,#]

[a] *Nuclear Medicine, IRCCS Ospedale Policlinico San Martino, Genova, Italy*
[b] *Department of Health Sciences (DISSAL), University of Genoa, Genova, Italy.*
[c] *Department of Experimental Medicine (DIMES), University of Genoa, Genova, Italy.*
[d] *Radiation Oncology, IRCCS Ospedale Policlinico San Martino, Genova, Italy.*
[e] *CNR, Institute of Molecular Bioimaging and Physiology (IBFM), Milano, Italy.*
[f] *Medical Oncology Unit 1, IRCCS Ospedale Policlinico San Martino, Genova, Italy*
[g] *Clinica di Oncologia Medica, IRCCS Ospedale Policlinico San Martino, Genova, Italy.*
[h] *Radiologic Unit, IRCCS Ospedale Policlinico San Martino, Genova, Italy*

ABSTRACT

The last version of the FIGO classification recommended imaging tools to complete the clinical assessment of patients with cervical cancer. However, the preferable imaging approach is still unclear. We aimed to explore the prognostic power of Magnetic Resonance Imaging (MRI), contrast-enhanced Computed Tomography (ceCT), and [^{18}F]-Fluorodeoxyglucose Positron Emission Tomography ([^{18}F]FDG-PET)/CT in patients staged for locally advanced cervical cancer (LACC, FIGO stages IB3-IVA). Thirty-six LACC patients (mean age 55.47 ± 14.01, range 31-82) were retrospectively enrolled. All of them underwent MRI, ceCT and [^{18}F]FDG-PET/CT before receiving concurrent chemoradiotherapy. A median dose of 45 Gy (range 42-50.4; 25-28 fractions, 5 fractions per week, 1 per day) was delivered through the external-beam radiation therapy (EBRT)

Correspondence to: Matteo Bauckneht, Nuclear Medicine, IRCCS Ospedale Policlinico San Martino, and Department of Health Sciences (DISSAL), University of Genoa, 16132 Genova, Italy, phone: +390105557360; fax: +390105556911.
E-mail address: matteo.bauckneht@unige.it (M. Bauckneht).
* Equally contributed as first coauthors.
** Equally contributed as last coauthors.

https://doi.org/10.1016/j.currproblcancer.2023.101007

on the pelvic area, while a median dose of 57.5 Gy (range 16-61.1; 25-28 fractions, 5 fractions per week, 1 per day) was administered on metastatic nodes. The median doses for brachytherapy treatment were 28 Gy (range 28-30; 4-5 fractions, 1 every other day). Six cycles of cisplatin or carboplatin were administered weekly. The study endpoints were recurrence-free survival (RFS) and overall survival (OS). Metastatic pelvic lymph nodes at MRI independently predicted RFS (HR 13.271, 95% CI 1.730-101.805; $P = 0.027$), while metastatic paraaortic lymph nodes at [^{18}F]FDG-PET/CT independently predicted both RFS (HR 11.734, 95% CI 3.200-43.026; $P = .005$) and OS (HR 13.799, 95% CI 3.378-56.361; $P < 0.001$). MRI and [^{18}F]FDG-PET/CT findings were incorporated with clinical evidences into the FIGO classification. With respect to the combination of clinical, MRI and ceCT data, the use of next-generation imaging (NGI) determined a stage migration in 10/36 (27.7%) of patients. Different NGI-based FIGO classes showed remarkably different median RFS (stage IIB: not reached; stage IIIC1: 44 months; stage IIIC2: 3 months; $P < 0.001$) and OS (stage IIB: not reached; stage IIIC1: not reached; stage IIIC2: 14 months; $P < 0.001$). A FIGO classification based on the combination of MRI and [^{18}F]FDG-PET/CT might predict RFS and OS of LACC patients treated with concurrent chemoradiotherapy.

ARTICLE INFO

Keywords: Positron emission tomography/computed tomography; Magnetic resonance imaging; Computed tomography; Locally advanced cervical cancer; FIGO stage; Recurrence-free survival; Overall survival

Introduction

Uterine cervical cancer represents a frequent malignancy in women worldwide, showing higher incidence and mortality rates in developing countries.[1] For this reason, the staging of this tumor is historically based on the purely clinical criteria of the Féderation Internationale de Gynécologie et d'Obstétrique (FIGO), while imaging findings were recommended to be added to the FIGO staging system only in the last update of this classification.[2]

Previous studies suggested that Magnetic resonance imaging (MRI) is the most accurate technique for the evaluation of the local extension of the lesion and for the identification of nodal or pelvic organs involvement[3-5] posing the bases for the increasing use of this technique in the routine clinical practice. However, both contrast-enhanced computed tomography (ceCT) and [^{18}F]-Fluorodeoxyglucose Positron Emission Tomography/Computed Tomography ([^{18}F]FDG PET/CT) can also be considered to assess paraaortic nodal involvement and the presence of distant metastases.[2,6]

In this scenario, it is not clear in which situations a combination of MRI with these techniques should be preferred for the primary staging of cervical cancer. Indeed, the addition of ceCT to MRI has been shown to provide a superior diagnostic accuracy than MRI alone for the detection of distant metastases,[5] while the combination of MRI and [^{18}F]FDG PET/CT seems to improve the detection of nodal involvement.[7] Verifying the prognostic power of imaging findings is mandatory to reinforce the role of next-generation imaging (NGI) in this clinical setting, potentially improving the level of evidence supporting its use.

Although not mandatory for the FIGO classification, [^{18}F]FDG PET/CT is commonly used in patients with locally advanced cervical cancer (LACC, corresponding to IB3-IVA FIGO stages), as it is the preferred tool for chemoradiotherapy treatment planning.[6,8-9] Thanks to its sensitivity, [^{18}F]FDG PET/CT may identify pathological nodes having a normal size at ceCT, thus guiding their irradiation, while it may rule out metabolically inactive enlarged lymph nodes, potentially avoiding futile toxicity. Therefore, LACC represents an ideal clinical scenario in which the risk stratification power of NGI in uterine cervical cancer can be measured.

In the present study, we retrospectively enrolled a naturalistic cohort of LACC patients submitted to MRI, ceCT, and [^{18}F]FDG PET/CT before receiving chemoradiotherapy plus endouterine

brachytherapy. The primary endpoint of the study was to test the prognostic value of a FIGO classification based on a multimodal imaging approach.

Materials and methods

Study population and study design

All patients with a histological diagnosis of squamous cell carcinoma (SCC) of the uterine cervix treated at our Institution between 2010 and 2020 were considered eligible for this retrospective study. Inclusion criteria were the following: (1) FIGO stages IB3-IVA; (2) MRI, ceCT and [^{18}F]FDG-PET/CT performed at baseline; and (3iii) treatment with concurrent chemoradiotherapy and simultaneous-integrated boost (SIB) guided by [^{18}F]FDG-PET/CT plus high dose rate endouterine brachytherapy boost. The retrospective analysis was conducted under the Declaration of Helsinki, Good Clinical Practice, and local ethical and legal regulations. The local ethical committee approved the retrospective monocentric study (CER Liguria 370/2022–DB id 12472). According to our standard procedure, all patients signed a written informed consent form, encompassing the use of anonymized data for retrospective research purposes before each imaging and therapeutic procedure.

Imaging procedures and data extraction from imaging reports

According to our Institutional protocol, MRI and ceCT were routinely performed according to current recommendations.[10,11]

MRI acquisition protocol

Pelvic MRI acquisitions were performed with a 1.5 T scanner (Magnetom AERA, Siemens, Munich, Germany). The administration of 20 mg hyoscine butyl bromide (Buscopan, Sanof SA, Paris, France) was used to reduce intestinal peristalsis. A phased array coil was used, and the sequences performed were as follows: axial T1 fast spin-echo, sagittal T2 fast recovery fast spin-echo (FRFSE), oblique axial T2 FRFSE, oblique axial T2 FRFSE, axial T2 FRFSE, axial diffusion-weighted sequences with 3 b values (0, 800, 1000 s/mm^2). Postcontrast imaging with axial T1 FSE was acquired 5 minutes after intravenous injection of gadolinium dimeglumine (Magnevist, Berlex, Wayne) 0.1 mol/L per kg body weight. Each MRI acquisition included an oblique axial T2 FRFSE (echo time [TE]), 102; repetition time [TR]), 3350; field of view [FOV], 26 cm, section thickness, 5 mm; spacing, 0 mm; and number of excitations [NEX], 3) and a sagittal T2 FRFSE sequences (TE, 85; TR, 3100; FOV, 24 cm; section thickness, 5 mm; spacing, 0.5 mm; and NEX, 4). ceCT of thorax, abdomen and pelvis was performed on a multidetector CT scanner (Siemens Definition Flash, Erlangen, Germany). As per the standard protocol, 120 kV and 160 mAs were used. Patients received 1 liter of water-soluble oral contrast 1 hour before the scan. Scanning was done immediately after intravenous injection of 80 mL of either Iohexol (Omnipaque 350, GE Healthcare, CA) or Iopamidol (Iomeron 400, Bracco, Italy). Images were reconstructed with 5 mm thickness at 5 mm interval.

[^{18}F]FDG-PET/CT acquisition protocol

[^{18}F]FDG-PET/CT imaging was performed following the European Association of Nuclear Medicine (EANM) guidelines[12] using PET/CT scanners fulfilling the EARL accreditation program. Integrated PET/CT scanners using either Hirez-Biograph 16 (Siemens Medical Solutions, Munich, Germany) or Biograph mCT Flow (Siemens Medical Solutions, Munich, Germany) were used to perform a whole-body (skull vertex to the upper thighs) PET acquisition in the 3-dimensional mode (emission time: 2 minutes per bed position with an axial field-of-view of 15.6 cm). A low-dose CT was performed for attenuation correction and anatomical allocation. Reconstruction was

performed with an ordered subset expectation maximization algorithm with 4 iterations per 8 subsets. Images were corrected for random coincidences and scatter.

Data extraction from imaging reports

Aiming to mimic the clinical practice, MRI, ceCT and [^{18}F]FDG-PET/CT imaging reports were reviewed in consensus by 2 experienced radiation oncologists. The following parameters were extracted from imaging reports: maximum diameter of the primary lesion (MRI), parametrial involvement (MRI), vaginal involvement (MRI), presence/absence of pelvic or paraaortic nodal metastases (either MRI, ceCT or [^{18}F]FDG-PET/CT).

Therapeutic procedures

Patients were treated with platinum-based chemotherapy concurrently with external beam radiotherapy (EBRT) and 3D image-guided brachytherapy (3D IGBT).[13] EBRT was delivered using 3DCRT, VMAT or IMRT techniques. The clinical target volume (CTV) was defined on the simulation CT scan, including cervical disease (CTV1) and external and internal iliac, obturator, inguinal, and paraaortic nodes (CTV2) if they were positive. The planning target volume (PTV) was defined by adding a 5 mm margin to the CTV. After completion of EBRT, patients underwent clinical and radiological assessments with a pelvic MRI to check the response at the cervical site before starting BT. EBRT was followed by 3D IGBT using high-dose-rate (HDR) (Microselectron HDR, Elekta, Sweden). Each brachytherapy session was performed with ultrasound guidance to ensure the appropriate positioning of the Fletcher CT/MR Applicator in the uterine cavity. The contouring of the GTV was performed according to GEC-ESTRO guidelines (Groupe Europeen de Curietherapie, European Society for Therapeutic Radiology and Oncology).[14,15] Treatment planning was performed using Oncentra Masterplan TCS V3.1.5 (Elekta, Stockholm, Sweden). Dose-volume histograms (DVHs) related to HR-CTV, IR-CTV, and OARs were evaluated, taking into account in particular: HR-CTV at the time of brachytherapy, IR-CTV, D90 HR-CTV and IR-CTV, and D2cc, D1cc, D0.1cc of the rectum, sigmoid, intestines, and bladder, urethra, as per GEC-ESTRO recommendations.[16,17]

The median EBRT dose prescribed was 45 Gy (range 42-50.4) given in 25-28 fractions (5 fractions per week, 1 per day) to the PTV1 on the pelvic area, and a median dose of 57.5 Gy (range 16-61.1) on NGI-based pathological nodes in 25-28 fractions (5 fractions per week, 1 per day). The median doses for brachytherapy treatment were 28 Gy (range 28-30) given in 4-5 fractions (6-7Gy/fraction/every other day) with a cumulative delivered dose between 80-90 Gy on the final high-risk CTV.[18,19] Chemotherapy usually consisted of either 6 cycles of cisplatin or carboplatin administered weekly during EBRT and BT.

Statistical analysis

The descriptive analyses were conducted using absolute frequency and percentage for categorical variables and by median and range for quantitative variables. Continuous data are expressed as mean $\pm$ SD. Differences were considered statistically significant when the p value (P) was <0.05.

The endpoints of the study were to measure the Relapse-Free Survival (RFS) and Overall Survival (OS) associated with MRI, ceCT, and [^{18}F]FDG PET/CT imaging findings. RFS and OS were measured from the date of treatment initiation to the date of the failure event. The failure event for RFS was defined as local or distant recurrence of the disease or death for any cause or last follow-up, while for OS it was defined as death due to any cause or last follow-up. Univariate and multivariate analyses were performed, assessing imaging findings in correlation with RFS and OS, using the Cox proportional hazard regression model, estimating hazard ratios (HRs) and their 95% confidence interval (CI). Only factors with a $P < 0.10$ at the univariable analysis were evaluated in the multivariable analyses.

Based on obtained findings, a FIGO staging system was obtained integrating the clinical assessment with the combination of MRI and [^{18}F]FDG-PET/CT (from now on termed "NGI-based FIGO"). The Kaplan–Meier method was used to estimate the survival curves of RFS and OS associated with each NGI-based FIGO class.[20] Stage migration was measured by creating the Sankey flow diagram.

All statistical analyses were performed using IBM-SPSS release 23 (IBM Corp. Released 2019. IBM SPSS Statistics for Windows, Version 26.0. Armonk, NY) and MedCalc release 12 (MedCalc Software, Mariakerke, Belgium).

Results

Patients' and treatment characteristics and clinical follow-up

Thirty-six patients (mean age 55.47 ± 14.01, range 31-82) satisfied the inclusion criteria and were retrospectively enrolled for the study. Patients' clinical, lab, imaging and treatment characteristics are summarized in Table 1. No patient at FIGO stage IVA was detected. All patients were assessable for survival analyses and were followed up for a median interval of 40 months (range 7-84). Among patients recruited, 14 (38.9%) experienced disease recurrence (median RFS 38 months, range 2-7), and 9 (25.3%) died during the clinical follow-up.

The prognostic power of MRI, ceCT, and [^{18}F]FDG-PET/CT imaging parameters

As detailed in Table 2, at the univariate analysis, the involvement of pelvic lymph nodes at MRI (HR 13.271, 95% CI 1.730-101.805) and the presence of [^{18}F]FDG-active pelvic and paraaortic lymph nodes (HR 5.267, 95% CI 1.174-23.634 and HR 11.734, 95% CI 3.200-43.026, respectively) resulted in significant predictors of the RFS ($P = 0.013$, $P = 0.030$, and $P < 0.001$, respectively). The multivariate analysis confirmed the presence of pathological pelvic lymph nodes at MRI and paraaortic lymph nodes at [^{18}F]FDG-PET/CT as independent predictors of the RFS ($P = 0.027$ and $P = 0.005$, respectively).

As detailed in Table 3, the univariate analysis identified the presence of pathological pelvic lymph nodes at MRI (HR 10.452, 95% CI 1.193-91.595) and of pelvic and paraaortic lymph nodes at [^{18}F]FDG-PET/CT as significant predictors of the OS (HR 6.915, 95% CI 0.859-55.671 and HR 13.799, 95% CI 3.378-56.361, respectively) ($P = 0.034$, $P = 0.069$, and $P < 0.001$, respectively). At the multivariate model, the presence of metastatic paraaortic lymph nodes at [^{18}F]FDG-PET/CT remained the sole independent prognosticator ($P < 0.001$).

Stage migration provided by NGI-based FIGO vs. FIGO classification

Based on the observed prognostic value of MRI and [^{18}F]FDG-PET/CT findings, we built the NGI-based FIGO classification, incorporating NGI in addition to the clinical assessment. Considering clinical, MRI and ceCT findings, patients were classified in the stages IIB (n = 14, 38.9%), IIIC1 (n = 14, 38.9%) and IIIC2 (n = 8, 22.2%). By contrast, considering NGI-based FIGO, 14 patients resulted at stage IIB (38.9%), 18 at stage IIIC1 (50%), and 4 at stage IIIC2 (11.1%). As displayed in Figure 1, 10 patients changed their stage when submitted to [^{18}F]FDG-PET/CT with respect to the classification based on MRI and ceCT. Molecular imaging up-staged 4 patients (from IIB to IIIC1), while 2 patients were down-staged from stage IIIC1 to the IIB group, 2 others from IIIC2 to IIB, and 2 more patients from IIIC2 to IIIC1.

Table 1
Patients' clinical, imaging, treatment and follow-up characteristics.

	Overall (n = 36)
Age	55.47 ± 14.01
Histological grading	
Grade 1	4 (11.1%)
Grade 2	10 (27.8%)
Grade 3	22 (61.1%)
HPV positivity	8 (22.2%)
Serum SCC antigen (ng/ml)	15.09 ± 23.61
Magnetic resonance imaging	
Primary lesion	
Maximal diameter < 4 cm	8 (22.2%)
Maximal diameter ≥ 4 cm	28 (77.8%)
Parametrial involvement	
Absent	3 (8.3%)
Unilateral	15 (41.7%)
Bilateral	18 (50.0%)
Vaginal involvement	
Absent	10 (27.8%)
Limited to the upper two-thirds	18 (50.0%)
Extended to the lower third	8 (22.2%)
Pelvic lymph node metastasis	15 (41.7%)
Contrast-enhanced computed tomography	
Paraaortic lymph node metastasis	8 (22.2%)
[^{18}F]FDG-PET/CT	
Pelvic lymph node metastasis	22 (61.1%)
Paraaortic lymph node metastasis	4 (11.1%)
Radiation therapy	
EBRT technique	
3D-CRT	2 (5.6%)
VMAT	13 (36.1%)
Helical IMRT	21 (58.3%)
Simultaneous-integrated boost	
Parametria	15 (41.7%)
Lymph nodes	4 (11.1%)
Both	17 (47.2%)
Total dose (Gy)	27.81 ± 1.65
Follow-up	
Relapse	14 (38.9%)
Death	9 (25.3%)

Abbreviations: [^{18}F]FDG-PET/CT, [^{18}F]-Fluorodeoxyglucose Positron Emission Tomography/Computed Tomography; 3D-CRT, 3-Dimensional Conformal Radiation Therapy; EBRT, External Beam Radiation Therapy; HPV, Human Papilloma Virus; IMRT, Intensity Modulated Radiation Therapy; SCC, Squamous Cell Carcinoma; VMAT, Volumetric Modulated Arc Therapy.

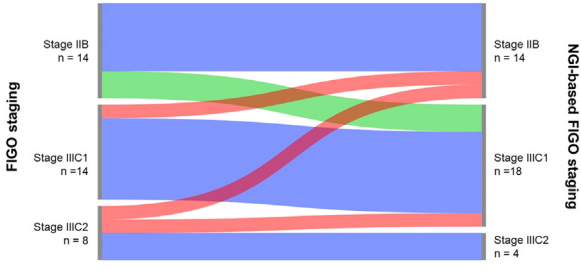

Fig. 1. Stage migration provided by NGI-based FIGO vs. FIGO classification: Sankey flow diagram. The Sankey flow diagram shows changes between the FIGO stages according to the multimodal imaging adopted: MRI plus ceCT (FIGO staging, left side) and MRI plus [^{18}F]FDG-PET/CT (NGI-based FIGO, right side). The green color highlights downstaging, while the red color highlights upstaging. (For interpretation of the references to colour in this figure legend, the reader is referred to the web version of this article.)

Table 2
Imaging parameters in the prediction of the RFS.

	Univariate analysis		Multivariate analysis	
	HR (95% CI)	*P* value	HR (95% CI)	*P* value
MRI				
Primary lesion				
T < 4 cm	1.000 (Ref)			
T ≥ 4 cm	1.911 (0.427-8.555)	0.397		
Parametrial involvement				
Absent	1.000 (Ref)			
Unilateral	0.755 (0.088-6.487)	0.797		
Bilateral	1.902 (0.235-15.378)	0.546		
Vaginal involvement				
Absent	1.000 (Ref)			
Upper two-thirds	1.561 (0.414-5.892)	0.511		
Lower third	1.555 (0.314-7.711)	0.589		
Pelvic N metastasis	13.271 (1.730-101.805)	**0.013**	10.282 (1.300-81.340)	**0.027**
ceCT				
Paraaortic N metastasis	1.887 (0.589-6.041)	0.285		
[^{18}F]FDG-PET/CT				
Pelvic N metastasis	5.267 (1.174-23.634)	**0.030**	1.708 (0.329-8.870)	0.524
Paraaortic N metastasis	11.734 (3.200-43.026)	**<0.001**	6.455 (1.746-23.867)	**0.005**

Univariate and multivariate analyses were performed with the Cox regression model. significant *P*-values are bolded. Abbreviations: [^{18}F]FDG-PET/CT, [^{18}F]-Fluorodeoxyglucose Positron Emission Tomography/Computed Tomography; ceCT, contrast-enhanced Computed Tomography; MRI, Magnetic Resonance Imaging; N, lymph node; T, primary lesion.

Table 3
Imaging parameters in the prediction of the OS.

	Univariate analysis		Multivariate analysis	
	HR (95% CI)	*P* value	HR (95% CI)	*P* value
MRI				
Primary lesion				
T < 4 cm	1.000 (Ref)			
T ≥ 4 cm	2.897 (0.358-23.444)	0.319		
Parametrial involvement				
Absent	1.000 (Ref)			
Unilateral	0.256 (0.050-1.326)	0.105		
Bilateral	1.469 (0.282-7.655)	0.648		
Vaginal involvement				
Absent	1.000 (Ref)			
Upper two-thirds	2.428 (0.270-21.852)	0.429		
Lower third	6.589 (0.729-59.511)	0.103		
Pelvic N metastasis	10.452 (1.193-91.595)	**0.034**	6.831 (0.667-69.941)	0.105
ceCT				
Paraaortic N metastasis	3.725 (0.794-13.954)	0.121		
[^{18}F]FDG-PET/CT				
Pelvic N metastasis	6.915 (0.859-55.671)	**0.069**	1.950 (0.168-22.587)	0.593
Paraaortic N metastasis	13.799 (3.378-56.361)	**<0.001**	13.799 (3.378-56.361)	**<0.001**

Univariate and multivariate analyses were performed with the Cox regression model. Significant *P*-values are bolded. Abbreviations: [^{18}F]FDG-PET/CT, [^{18}F]-Fluorodeoxyglucose Positron Emission Tomography/Computed Tomography; ceCT, contrast-enhanced Computed Tomography; MRI, Magnetic Resonance Imaging; N, lymph node; T, primary lesion.

The prognostic power of the NGI-based FIGO staging

In NGI-based FIGO stage IIB, recurrence occurred in 2 patients (14.2%) and just 1 patient died (7.1%). In the IIIC1 group, 8 patients experienced recurrence (44.4%), and 4 deaths were observed (22.2%). All patients belonging to stage IIIC2 experienced recurrence and died. Kaplan–Meier curves demonstrated that patients grouped according to NGI-based FIGO classification showed

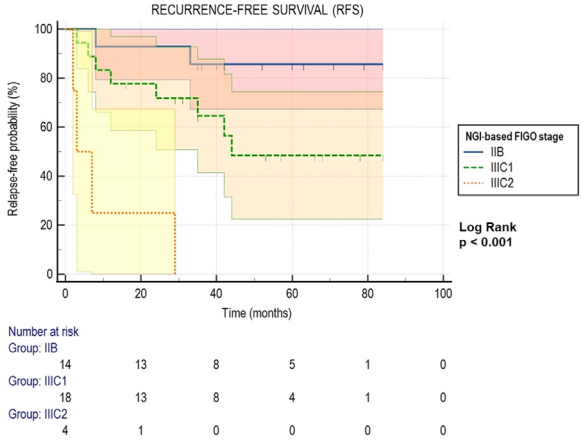

Fig. 2. Kaplan–Meier curves for RFS. Kaplan–Meier curves for the relapse-free survival (RFS) in patients grouped by NGI-based FIGO classification.

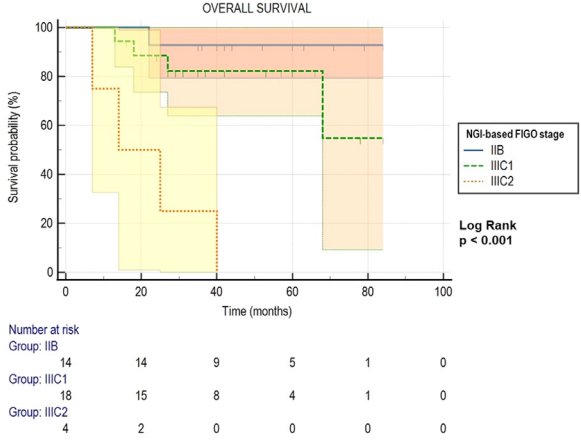

Fig. 3. Kaplan–Meier curves for OS. Kaplan–Meier curves for the overall survival (OS) in patients grouped by NGI-based FIGO classification.

significant differences in terms of median RFS (mRFS; $P < 0.001$) (Fig 2). In particular, mRFS was 3 months (95% CI 2-29) and 44 months (95% CI 24-44) for the stages IIIC2 and IIIC1, respectively. mRFS was not reached in group IIB.

Median OS (mOS) was significantly different between the NGI-based FIGO stages ($P < 0.001$) (Fig 3). Patients at stage IIIC2 had a mOS of 14 months (95% CI 7-40), while in the 2 remaining groups mOS was not reached.

Discussion

Given that most cervical cancer patients live in underdeveloped or developing countries that lack healthcare resources, studies assessing the risk stratification power of NGI, its impact on the subsequent clinical management and, ultimately, the impact on the oncological outcome of its use, would provide helpful information for policy decision-making and clinical practice.

In the present study, the local assessment of LACC through MRI resulted in an independent predictor of the RFS, in line with the well-known superiority of MRI compared to other imaging techniques in the locoregional assessment of both the primary lesion and the pelvic lymph nodes.[3-5] Similarly, confirming previous evidence,[21,22] our results showed that the presence of metastatic paraaortic lymph nodes at [^{18}F]FDG-PET/CT independently predicts RFS and OS. By contrast, the detection of distant metastatic lymph nodes by ceCT did not show any prognostic value in our sample. Indeed, taking into account [^{18}F]FDG-PET/CT over ceCT in addition to MRI for the definition of the FIGO staging, provided a stage migration in roughly 25% of enrolled patients. Due to the study design, and in agreement with international guidelines [8], all enrolled patients received [^{18}F]FDG-PET/CT-guided SIB. This prevented the possibility to compare the oncological outcome of conventional imaging-based with NGI-based FIGO classes. However, we presume that refining the staging system may improve treatment outcomes for upstaged patients and reduce unnecessary toxicity for down-staged ones. Future studies with prospective and possibly randomized designs are needed to address this point.

A similar consideration applies to the observed prognostic power of the NGI-based FIGO staging system. Although it needs to be validated by further studies on larger and independent populations, it improves the current knowledge of imaging parameters in relation to clinical outcomes and supports the implementation of NGI in the LACC clinical practice. Should this finding be confirmed, [^{18}F]FDG-PET/CT should be preferred to ceCT in combination with MRI for the NGI-based primary staging of LACC, as already suggested (though not formally recommended) by international guidelines.[23]

The present study has several limitations. The first is the relatively small sample size. However, its monocentric design guarantees a homogeneous multidimensional assessment of our patients. Moreover, imaging findings were qualitatively extracted from imaging reports. This choice prevented our capability to assess the eventual added value of quantitative imaging parameters in the risk stratification of LACC patients, as previously assessed by several studies.[21,24-28] However, from a practice-oriented perspective, we aimed to mimic the clinical scenario, in which the staging process is made by clinicians after collecting radiologists' and nuclear medicine physicians' reports. The concept that qualitative imaging findings, obtained by the treating physician by reading imaging reports improve the risk assessment of LACC further supports the implementation of NGI in clinical practice. Furthermore, recruited patients were treated in a relatively large time span (from 2010-2020). Even if just few minor modifications to treatment protocols occurred,[29] this might have theoretically an impact on the oncological outcome. However, only prospective trials confirming our results could clarify this issue. Finally, according to the NGI-based FIGO classification, no patient resulted at the stages IIIA and IIIB. This result might depend on the sensitivity of the NGI assessment of nodes' involvement.[7] However, we cannot exclude that this finding might be influenced by the small 4 sample size of the study.

In conclusion, the combination of MRI and [^{18}F]FDG-PET/CT might improve the prediction of RFS and OS in patients with LACC at stages IIB-IIIC2 treated with concurrent chemoradiotherapy, endouterine brachytherapy boost and [^{18}F]FDG-PET/CT-guided SIB. Despite a limited sample size, our data suggest that extending this multimodal approach in the management of LACC may improve the pre-treatment risk stratification. Further studies in larger and independent samples are necessary to validate these results. However, if confirmed, these findings could be helpful to determine which multimodal imaging approach should be preferable in the staging of cervical cancer.

Author contributions

Conceptualization: SR, FL, LB, CS, MB; Ethical committee protocol submission: AST; data collection: SR, FL, CS, LB, SMo, GMS, CM, SB, AL, AST, SMa; statistical analysis: FL, MB; writing-original draft preparation: FL, MB; writing-review and editing: all coauthors. All authors have read and agreed to the published version of the manuscript.

Ethics approval

The local ethical committee approved the retrospective monocentric study (CER Liguria 370/2022-DB id 12472).

Consent to participate

All patients enrolled in the study signed a written informed consent at the time of imaging, encompassing the use of anonymized data for retrospective research purposes.

Availability of data and material

The data that support the findings of this study are available from the corresponding author upon reasonable request.

Declaration of Competing Interest

The authors declare that they have no known competing financial interests or personal relationships that could have appeared to influence the work reported in this paper.

References

1. Sung H, Ferlay J, Siegel RL, Laversanne M, Soerjomataram I, Jemal A, Bray F. Global Cancer Statistics 2020: GLOBOCAN estimates of incidence and mortality worldwide for 36 cancers in 185 countries. *CA Cancer J Clin*. 2021. doi:10.3322/caac.21660.
2. Bhatla N, Berek JS, Cuello Fredes M, et al. Revised FIGO staging for carcinoma of the cervix uteri. *Int J Gynaecol Obstet*. 2019. doi:10.1002/ijgo.12749.
3. Balleyguier C, Sala E, Da Cunha T, et al. Staging of uterine cervical cancer with MRI: guidelines of the European Society of Urogenital Radiology. *Eur Radiol*. 2011. doi:10.1007/s00330-010-1998-x.
4. Bhosale P, Peungjesada S, Devine C, Balachandran A, Iyer R. Role of magnetic resonance imaging as an adjunct to clinical staging in cervical carcinoma. *J Comput Assist Tomogr*. 2010. doi:10.1097/RCT.0b013e3181ed3090.
5. Bipat S, Glas AS, van der Velden J, Zwinderman AH, Bossuyt PM, Stoker J. Computed tomography and magnetic resonance imaging in staging of uterine cervical carcinoma: a systematic review. *Gynecol Oncol*. 2003. doi:10.1016/s0090-8258(03)00409-8.
6. Cibula D, Pötter R, Planchamp F, et al. The European Society of Gynaecological Oncology/European Society for Radiotherapy and Oncology/European Society of Pathology Guidelines for the management of patients with cervical cancer. *Int J Gynecol Cancer*. 2018. doi:10.1097/IGC.0000000000001216.
7. Choi HJ, Ju W, Myung SK, Kim Y. Diagnostic performance of computer tomography, magnetic resonance imaging, and positron emission tomography or positron emission tomography/computer tomography for detection of metastatic lymph nodes in patients with cervical cancer: meta-analysis. *Cancer Sci*. 2010. doi:10.1111/j.1349-7006.2010.01532.x.
8. Adam JA, Loft A, Chargari C, et al. EANM/SNMMI practice guideline for [18F]FDG PET/CT external beam radiotherapy treatment planning in uterine cervical cancer v1.0. *Eur J Nucl Med Mol Imaging*. 2021. doi:10.1007/s00259-020-05112-2.
9. Haie-Meder C, Mazeron R, Magné N. Clinical evidence on PET-CT for radiation therapy planning in cervix and endometrial cancers. *Radiother Oncol*. 2010. doi:10.1016/j.radonc.2010.07.010.
10. Manganaro L, Lakhman Y, Bharwani N, et al. Staging, recurrence and follow-up of uterine cervical cancer using MRI: updated guidelines of the European Society of Urogenital Radiology after revised FIGO staging 2018. *Eur Radiol*. 2021. doi:10.1007/s00330-020-07632-9.
11. Kaur H, Silverman PM, Iyer RB, Verschraegen CF, Eifel PJ, Charnsangavej C. Diagnosis, staging, and surveillance of cervical carcinoma. *AJR Am J Roentgenol*. 2003. doi:10.2214/ajr.180.6.1801621.
12. Boellaard R, Delgado-Bolton R, Oyen WJ, et al. FDG PET/CT: EANM procedure guidelines for tumour imaging: version 2.0. *Eur J Nucl Med Mol Imaging*. 2015. doi:10.1007/s00259-014-2961-x.
13. Rose PG, Bundy BN, Watkins EB, et al. Concurrent cisplatin-based radiotherapy and chemotherapy for locally advanced cervical cancer. *N Engl J Med*. 1999. doi:10.1056/NEJM199904153401502.
14. International Commission on Radiation Units and MeasurementsPrescribing, recording, and reporting brachytherapy for cancer of the cervix. *J ICRU*. 2013. doi:10.1093/jicru/ndw027.
15. Haie-Meder C, Pötter R, Van Limbergen E, et al. Recommendations from Gynaecological (GYN) GEC-ESTRO Working Group (I): concepts and terms in 3D image based 3D treatment planning in cervix cancer brachytherapy with emphasis on MRI assessment of GTV and CTV. *Radiother Oncol*. 2005. doi:10.1016/j.radonc.2004.12.015.

16. Mahantshetty U, Poetter R, Beriwal S, et al. IBS-GEC ESTRO-ABS recommendations for CT based contouring in image guided adaptive brachytherapy for cervical cancer. *Radiother Oncol*. 2021. doi:10.1016/j.radonc.2021.05.010.
17. Dimopoulos JC, Petrow P, Tanderup K, et al. Recommendations from gynaecological (GYN) GEC-ESTRO working group (IV): basic principles and parameters for MR imaging within the frame of image based adaptive cervix cancer brachytherapy. *Radiother Oncol*. 2012. doi:10.1016/j.radonc.2011.12.024.
18. Viswanathan AN, Thomadsen BAmerican Brachytherapy Society Cervical Cancer Recommendations Committee; American Brachytherapy Society. American Brachytherapy Society consensus guidelines for locally advanced carcinoma of the cervix. Part I: general principles. *Brachytherapy*. 2012. doi:10.1016/j.brachy.2011.07.003.
19. Viswanathan AN, Beriwal S, De Los Santos JF, et al. American Brachytherapy Society consensus guidelines for locally advanced carcinoma of the cervix. Part II: high-dose-rate brachytherapy. *Brachytherapy*. 2012. doi:10.1016/j.brachy.2011.07.002.
20. Kaplan EL, Meier P. Nonparametric estimation from incomplete observations. *J Am Stat Asso*. 1958. doi:10.2307/2281868.
21. Liu FY, Lai CH, Yang LY, et al. Utility of (18)F-FDG PET/CT in patients with advanced squamous cell carcinoma of the uterine cervix receiving concurrent chemoradiotherapy: a parallel study of a prospective randomized trial. *Eur J Nucl Med Mol Imaging*. 2016. doi:10.1007/s00259-016-3384-7.
22. Kidd EA, Siegel BA, Dehdashti F, Rader JS, Mutch DG, Powell MA, Grigsby PW. Lymph node staging by positron emission tomography in cervical cancer: relationship to prognosis. *J Clin Oncol*. 2010. doi:10.1200/JCO.2009.25.4151.
23. National Comprehensive Cancer Network. *NCCN Clinical Practice Guidelines in Oncology: Cervical Cancer (Version 1.2023)*; 2023. Available from: https://www.nccn.org/professionals/physician_gls/pdf/cervical.pdf. Accessed 7 January 2023.
24. Cho HW, Lee ES, Lee JK, Eo JS, Kim S, Hong JH. Prognostic value of textural features obtained from F-fluorodeoxyglucose (F-18 FDG) positron emission tomography/computed tomography (PET/CT) in patients with locally advanced cervical cancer undergoing concurrent chemoradiotherapy. *Ann Nucl Med*. 2023. doi:10.1007/s12149-022-01802-z.
25. de Alencar NRG, Machado MAD, Mourato FA, et al. Exploratory analysis of radiomic as prognostic biomarkers in 18F-FDG PET/CT scan in uterine cervical cancer. *Front Med (Lausanne)*. 2022. doi:10.3389/fmed.2022.1046551.
26. Han L, Wang Q, Zhao L, Feng X, Wang Y, Zou Y, Li Q. A systematic review and meta-analysis of the prognostic impact of pretreatment fluorodeoxyglucose positron emission tomography/computed tomography parameters in patients with locally advanced cervical cancer treated with concomitant chemoradiotherapy. *Diagnostics (Basel)*. 2021. doi:10.3390/diagnostics11071258.
27. Han S, Kim H, Kim YJ, Suh CH, Woo S. Prognostic value of volume-based metabolic parameters of 18F-FDG PET/CT in uterine cervical cancer: a systematic review and meta-analysis. *AJR Am J Roentgenol*. 2018. doi:10.2214/AJR.18.19734.
28. Ramlov A, Kroon PS, Jürgenliemk-Schulz IM, et al. Impact of radiation dose and standardized uptake value of (18)FDG PET on nodal control in locally advanced cervical cancer. *Acta Oncol*. 2015. doi:10.3109/0284186X.2015.1061693.
29. Sagae S, Toita T, Matsuura M, et al. Improvement in radiation techniques for locally advanced cervical cancer during the last two decades. *Int J Gynecol Cancer*. 2023. doi:10.1136/ijgc-2022-004230.